American Mineralogist, Volume 74, pages 870–876, 1989

Structural variations in natural F, OH, and Cl apatites

JOHN M. HUGHES, MARYELLEN CAMERON, KEVIN D. CROWLEY
Department of Geology, Miami University, Oxford, Ohio 45056, U.S.A.

ABSTRACT

The crystal structures of the hexagonal ($P6_3/m$) end-member apatites with the formula $Ca_5(PO_4)_3X$ (X = F, OH, Cl) were refined to $R = 0.025$, 0.016, and 0.020 for fluorapatite, hydroxylapatite, and chlorapatite, respectively. In accord with earlier studies, the F atoms in fluorapatite lie in the mirror plane in the $2a$ (0,0,¼) special position. In hydroxylapatite, the OH species is disordered in (0,0,z) positions 0.35 Å above and below the mirror plane, and in chlorapatite the Cl is also disordered, in positions 1.2 Å above and below the mirror planes. In chlorapatite, the Cl anion is so far displaced from the mirror plane that an additional, weak bond develops between Ca(2) and a second Cl anion, thus increasing the Ca(2) coordination.

In the three end-members, differences in position of the column anions propagate throughout the structure, but have minor, secondary effects on the $Ca(1)O_9$ polyhedron and the PO_4 tetrahedron in terms of cation-oxygen bond lengths and polyhedron orientation; average P–O and average Ca(1)–O bond lengths for the three structures are identical within 0.005 Å. The $Ca(2)O_5X(O)$ polyhedron, however, is greatly affected by anion substitution. Individual Ca(2)–X bond lengths are significantly different for the three structures, with the Ca(2)–X bond length varying between 2.311 and 2.759 Å. The mean Ca(2)–O distance ranges between 2.461 and 2.493 Å.

The atomic arrangements of fluorapatite, hydroxylapatite, and chlorapatite suggest that these end-members are immiscible in solid solution. The 1.2-Å displacement of Cl from the mirror plane in chlorapatite prohibits the existence of F and OH as immediate neighbors at certain sites in the anion columns because of prohibitively short interatomic distances. Structural adjustments that enable solid solution to occur in Cl-bearing binary or ternary apatites may include (1) major shifts in column-anion positions compared to those in end-member structures, (2) reduction of symmetry from hexagonal to monoclinic in ternary apatites, and/or (3) ordering of anions within individual columns but disordering of columns throughout the apatite structure.

INTRODUCTION

Natural apatites of composition $Ca_5(PO_4)_3(F,OH,Cl)$ exhibit large variations in F, Cl, and OH contents. Pure end-members are uncommon in nature, but binary and ternary compositions are widely reported in igneous, metamorphic, and sedimentary rocks. Petrologists have proposed that the F-Cl-OH variations in apatites are potential geothermometers (e.g., Stormer and Carmichael, 1971) and indicators of volatile fugacities in magmatic and hydrothermal processes (e.g., Candela, 1986; Boudreau and McCallum, 1987). Other recent studies have shown that F, OH, and Cl concentrations correlate directly with properties such as etching rates and annealing characteristics of U fission tracks in apatite (e.g., Green et al., 1986; Crowley and Cameron, 1987).

Despite the ubiquitous nature of apatite minerals and their potential usefulness as petrogenetic indicators, relatively few structure studies of natural crystals have been undertaken. The $P6_3/m$ fluorapatite structure was described more than 50 years ago (Náray-Szabó, 1930; Mehmel, 1930), and the most recent modern refinements of the end-members were published in the early 1970s, i.e., $P2_1/b$ synthetic chlorapatite by Mackie et al. (1972), $P2_1/b$ synthetic hydroxylapatite by Elliott et al. (1973), and $P6_3/m$ synthetic and natural fluorapatite by Sudarsanan et al. (1972).

In this paper, we report three new structure refinements on natural $P6_3/m$ near–end-member fluorapatite, chlorapatite, and hydroxylapatites (binary and ternary apatites will be described in a subsequent paper). These structures differ from those of their synthetic counterparts, perhaps as a result of differences in anion ordering caused by impurities and vacancies. The structural differences between synthetic and natural crystals, and between end-member and binary or ternary species, warrant careful consideration where apatites are used in thermodynamic, diffusion, fission-track, and partitioning studies.

EXPERIMENTAL DETAILS

Near–end-member specimens from several well-documented localities were chosen for study. The specimen of fluorapatite is from Durango, Mexico (Young et al., 1969). Electron-microprobe analysis and instrumental neutron

0003–004X/89/0708–0870$02.00

TABLE 1. Crystal data and results of crystal-structure refinements for fluorapatite, hydroxylapatite, and chlorapatite

	F	OH	Cl
Crystal size (mm)	0.08 × 0.13 × 0.16	0.25 × 0.20 × 0.10	0.35 × 0.25 × 0.20
Unit-cell dimensions			
Least squares			
a (Å)	9.398(3)	9.418(2)	9.598(2)
b (Å)	9.397(3)	9.416(2)	9.598(2)
c (Å)	6.878(2)	6.875(2)	6.776(4)
α (°)	89.99(2)	90.01(3)	89.97(3)
β (°)	90.02(2)	89.99(2)	90.02(3)
γ (°)	120.06(2)	119.94(2)	119.96(2)
Structure refinement			
a	9.3973	9.4166	9.5979
c	6.8782	6.8745	6.7762
Reflections	1197	1201	1243
Unique reflections	379	383	397
R_{merge}	0.014	0.012	0.010
Reflections $I > 3\sigma_I$	328	344	354
R	0.025	0.016	0.020
R_w	0.029	0.022	0.028
$\Delta\rho$ residua (e Å^{-3})			
+	0.388	0.333	0.326
−	0.745	0.332	0.374

Note: Numbers in parentheses denote one esd of the least-significant digit.

activation analysis (INAA) yielded a composition of $(Ca_{4.90}Fe_{0.01}Sr_{0.01}Ce_{0.02})_{\Sigma 4.94}(P_{2.96}Si_{0.02}S_{0.03})_{\Sigma 3.01}O_{12}(F_{0.94}Cl_{0.08})_{\Sigma 1.02}$. Hydroxylapatite is represented by a specimen from Holly Springs, Georgia (National Museum of Natural History no. R-9498); analysis of this specimen by electron microprobe and INAA gave a composition of $Ca_{4.98}P_{2.99}O_{12}(F_{0.06}Cl_{0.03}OH_{0.91})_{\Sigma 1.00}$. The OH content was determined by difference. The chlorapatite specimen is from Kragero, Norway (American Museum of Natural History no. 23101), and yielded a composition of $(Ca_{4.88}Fe_{0.01}Na_{0.08}Ce_{0.01})_{\Sigma 4.98}P_{3.01}O_{12}(F_{0.09}Cl_{0.88})_{\Sigma 0.97}$ by electron-microprobe and INAA analysis.

Crystals were examined under plane-polarized light to insure that each specimen selected was an untwinned single crystal. Preliminary precession studies were undertaken, using a, b, and [110] axis photographs, to confirm that monoclinic superstructure reflections were not present and to verify the quality of X-ray diffraction maxima.

X-ray data for all crystals were measured using an Enraf-Nonius CAD4 single-crystal diffractometer and graphite-monochromated Mo$K\alpha$ radiation. Unit-cell parameters were refined (no symmetry constraints) using diffraction angles from 25 automatically centered reflections. Refined parameters and the idealized hexagonal parameters (idealized as per Frenz, 1985) used for structure refinement are given in Table 1.

Data were collected from a quadrant of reciprocal space to 52° 2θ. Intensities were measured using a $\theta/2\theta$ scan technique, with scan widths determined by the relationship $\omega = 1.00° + 0.34 \tan\theta$, to correct for dispersion of the Mo$K\alpha$ spectrum. Regularly interspersed intensity and orientation standards were monitored throughout data collection. A prescan of each peak during data collection determined counting time, with a maximum of 90 s per reflection. One-third of the total counting time was spent determining background on both sides of the peak.

Data were reduced and corrected for Lorentz and polarization effects. Absorption effects were corrected using an empirical psi-scan technique, using data obtained from 360° psi scans. Equivalent reflections were then merged; reflections with $I < 3\sigma_I$ were considered unobserved (Table 1).

Crystal-structure calculations were undertaken in space group $P6_3/m$ using the SDP-Plus set of programs (Frenz, 1985). Full-matrix least-squares refinement was undertaken by refining positional parameters, scale factor, anisotropic temperature factors, and an isotropic extinction factor. Weights proportional to σ_I^{-2} were assigned to individual structure factors with a term to downweight the contribution of intense reflections. Neutral-atom scattering factors, including terms for anomalous dispersion, were used in the refinement.

For fluorapatite, starting parameters were taken from Sudarsanan (1972); occupancy of the halogens was modeled with 95% F, located on the mirror plane at (0,0,¼), and 5% Cl, constrained to lie at the Cl position obtained in the chlorapatite structure refinement. For hydroxylapatite, refinement was initiated using the parameters in the fluorapatite study, although some symmetry constraints were released. It was assumed that the OH ions were disordered along c about the mirror plane at $z = ¼$ and that the hydroxyl O and H atoms were located in a half-occupied (0,0,z) position, necessary in a $P6_3/m$ apatite. The H positional parameter was refined, but the anisotropic temperature factors were fixed at those derived from the neutron-diffraction data of Kay et al. (1964). The crystal-structure refinement of chlorapatite was undertaken using starting parameters from Mackie et al. (1972);

TABLE 2. Positional parameters and equivalent isotropic temperature factors (Å²) for end-member apatites

	x*	y	z	B (Å²)
Ca(1)				
F	⅔	⅓	0.0010(1)	0.91(1)
OH	⅔	⅓	0.00144(8)	0.929(7)
Cl	⅔	⅓	0.0027(1)	0.99(1)
Ca(2)				
F	−0.00712(7)	0.24227(7)	¼	0.77(1)
OH	−0.00657(5)	0.24706(5)	¼	0.859(9)
Cl	0.00112(6)	0.25763(6)	¼	1.14(1)
P				
F	0.36895(8)	0.39850(8)	¼	0.57(1)
OH	0.36860(6)	0.39866(6)	¼	0.62(1)
Cl	0.37359(7)	0.40581(7)	¼	0.77(1)
O(1)				
F	0.4849(2)	0.3273(3)	¼	0.99(4)
OH	0.4850(2)	0.3289(2)	¼	1.00(3)
Cl	0.4902(2)	0.3403(2)	¼	1.34(4)
O(2)				
F	0.4667(2)	0.5875(3)	¼	1.19(5)
OH	0.4649(2)	0.5871(2)	¼	1.25(3)
Cl	0.4654(2)	0.5908(2)	¼	1.47(4)
O(3)				
F	0.2575(2)	0.3421(2)	0.0705(2)	1.32(3)
OH	0.2580(1)	0.3435(1)	0.0703(2)	1.57(2)
Cl	0.2655(2)	0.3522(2)	0.0684(3)	1.88(3)
X				
F	0	0	¼	1.93(6)
O(H)	0	0	0.1979(6)	1.31(8)
H	0	0	0.04(2)	3.3
Cl	0	0	0.4323(4)	2.68(5)

Note: Numbers in parentheses denote one esd of the least-significant digit.

halogen occupancy was modeled with 0.86 atoms of Cl disordered in a (0,0,*z*) position and 0.11 F atoms fixed at (0,0,¼), in accord with the microprobe data.

Data-collection procedures and the results of the refinements are summarized in Table 1. Table 2 contains positional parameters and equivalent isotropic *B* values for the end-member apatites, and Table 3 records anisotropic thermal parameters for atoms in the three structures. Table 4 contains bond lengths and angles for the three polyhedra of the end-member structures. In this case, the term "bond angle" is defined as the angle that each cation-anion bond makes with each of the unit cell axes. This usage is meant to facilitate comparison among the structures by providing a common reference system. Table 5[1] contains observed and calculated structure factors for the three structures.

STRUCTURAL VARIATIONS IN FLUORAPATITE, HYDROXYLAPATITE, AND CHLORAPATITE

A detailed description of the $P6_3/m$ apatites was provided by Beevers and McIntyre (1946). For the purposes of this paper, we regard the structure as being made up of Ca(1) and Ca(2) coordination polyhedra hexagonally disposed about a central [001] hexad (Fig. 1). The F, Cl, and OH ions lie in columns on these hexads at (0,0,*z*)

[1] A copy of Table 5 may be ordered as Document AM-89-412 from the Business Office, Mineralogical Society of America, 1625 I Street, N.W., Washington, D.C. 20006, U.S.A. Please remit $5.00 in advance for the microfiche.

TABLE 3. Anisotropic thermal parameters (Å²) for atoms in end-member apatites

	β_{11}	β_{22}	β_{33}	β_{12}	β_{13}	β_{23}
Ca(1)						
F	0.00394(6)*	0.00394	0.0033(1)	0.00394	0	0
OH	0.00408(5)	0.00408	0.0033(1)	0.00408	0	0
Cl	0.00462(6)	0.00462	0.0023(2)	0.00462	0	0
Ca(2)						
F	0.00256(6)	0.00361(6)	0.0034(1)	0.00299(9)	0	0
OH	0.00308(5)	0.00353(5)	0.00417(8)	0.00312(7)	0	0
Cl	0.00449(6)	0.00526(6)	0.0037(1)	0.00456(8)	0	0
P						
F	0.00208(7)	0.00231(7)	0.0032(1)	0.0025(1)	0	0
OH	0.00223(5)	0.00250(6)	0.0034(1)	0.00254(8)	0	0
Cl	0.00310(6)	0.00330(6)	0.0034(1)	0.00368(9)	0	0
O(1)						
F	0.0037(2)	0.0044(2)	0.0055(4)	0.0053(3)	0	0
OH	0.0036(2)	0.0044(2)	0.0059(3)	0.0054(2)	0	0
Cl	0.0059(2)	0.0075(2)	0.0054(4)	0.0102(3)	0	0
O(2)						
F	0.0038(2)	0.0030(2)	0.0088(5)	0.0028(3)	0	0
OH	0.0035(2)	0.0031(2)	0.0105(3)	0.0032(2)	0	0
Cl	0.0049(2)	0.0036(2)	0.0109(5)	0.0040(3)	0	0
O(3)						
F	0.0043(2)	0.0077(2)	0.0055(3)	0.0076(2)	−0.0032(4)	−0.0052(5)
OH	0.0050(1)	0.0096(1)	0.0070(2)	0.0101(2)	−0.0050(3)	−0.0082(3)
Cl	0.0062(1)	0.0113(2)	0.0076(3)	0.0119(2)	−0.0070(4)	−0.0109(5)
X						
F	0.0029(3)	0.0029	0.022(1)	0.0029	0	0
O(H)	0.0030(3)	0.0030	0.012(1)	0.0030	0	0
Cl	0.0056(1)	0.0056	0.027(1)	0.0056	0	0

Note: The form of the anisotropic temperature factor is exp $-[\beta_{11}h^2 + \beta_{22}k^2 + \beta_{33}l^2 + \beta_{12}hk + \beta_{13}hl + \beta_{23}kl]$. Numbers in parentheses denote one esd of the least-significant digit.

positions. The Ca(1) polyhedron is nine-coordinated, with six shorter bonds that define an approximate trigonal prism and three longer Ca(1)–O(1) bonds that emerge through the prism faces. The $Ca(1)O_9$ polyhedra share (001) pinacoid faces to form chains parallel to *c*. The Ca(2) polyhedron can be considered to be a CaO_5X octahedron, but a seventh weak bond to O(1) (0.15 valence units) exists in fluorapatite and hydroxylapatite, redefining the polyhedron as $CaO_5X(O)$. The Ca(2) atoms within mirror planes at $z = 0.25$ and 0.75 form triangles that are centered around the [001] zone axes containing the X anions. Adjacent Ca(1) and Ca(2) polyhedra are linked through oxygen atoms shared with PO_4 tetrahedra.

Cation polyhedra

Changes induced in the natural apatites as a result of differences in the column anion propagate throughout the crystal structure. The effects on the $Ca(1)O_9$ polyhedra and the PO_4 tetrahedra are minor, whereas those on the $Ca(2)O_5X(O)$ polyhedron are significant.

Phosphate tetrahedra for the three structures are compared in the ORTEP (Johnson, 1965) plot of Figure 2. As seen in that figure and Table 4, differences in anion content effect only minor changes in both interatomic distances and angles of the tetrahedra. Sets of analogous bond lengths for the three structures differ by a maximum of 0.008 Å. Analogous O–P–O angles exhibit variations on the order of 0.1–1.1°. Among the three structures, average bond lengths vary within a range of only 0.005 Å. Differences of approximately 1° in the angular disposition of the P–O(1) and P–O(2) bonds with respect to the *a* and *b* axes (Table 4) may reflect the slight displacement of Ca(2) induced by changes in position of the column anion.

The $Ca(1)O_9$ polyhedra in the end-member apatite structures also show little response to anion substitution, as documented in Figure 2 and Table 4. The largest range in individual Ca–O bonds involves Ca(1)–O(3), which exhibits a variation of 0.014 Å among the three structures. Average bond lengths for the Ca(1) polyhedra of the three apatites differ by only 0.005 Å. Small (~1–3°) deviations in orientations of bonds with respect to the crystallographic axes result from small differences in the *z* parameter of Ca(1) in the three structures.

The major structural response to anion substitution in the natural end-member apatites studied occurs in the $Ca(2)O_5X(O)$ polyhedron (Fig. 2 and Table 4). Large differences in position of the column anion (F, Cl, OH species) are especially evident in Figure 2. Individual Ca(2)–X bond lengths are significantly different for the three structures, with the Ca(2)–X bond length varying between 2.311 and 2.759 Å (Table 4). The Ca(2)–O(1) bond length is similar in fluorapatite and hydroxylapatite (2.70 and 2.71 Å, respectively), but is 0.20 Å longer in chlorapatite.

Geometry of the column-anion positions

The column anions in the three natural apatites examined in this study lie on [001] hexads. The F anions lie in the 2*a* special position at the intersection of the hexads and mirror planes at $z = 0.25$ and 0.75. Each F is bonded to three Ca(2) atoms that form a triangle within the mirror plane. The OH anions are disordered 0.35 Å above or below the mirror planes, and Cl ions are disordered 1.2 Å above or below the planes. The disordering of Cl and OH from the 2*a* special position reflects the structural accommodation required between the column anion and the triangle of Ca(2) atoms. The Ca(2)–Ca(2) distances (and areas of the corresponding triangle) vary from 4.002 Å (6.94 Å²) to 4.084 Å (7.22 Å²) to 4.273 Å

TABLE 4. Bond lengths (Å) and angles (°) with unit-cell axes for cation polyhedra in end-member apatites

	F	OH	Cl
P^A–$O(1)^A$	1.537(3) Å	1.534(2) Å	1.533(3) Å
a–P^A–$O(1)^A$	22.14°	21.78°	20.80°
b–P^A–$O(1)^A$	142.14°	141.78°	140.80°
c–P^A–$O(1)^A$	90°	90°	90°
P^A–$O(2)^A$	1.539(2) Å	1.537(2) Å	1.538(2) Å
a–P^A–$O(2)^A$	88.86°	89.26°	90.25°
b–P^A–$O(2)^A$	31.14°	30.74°	29.75°
c–P^A–$O(2)^A$	90°	90°	90°
P^A–$O(3)^{A,J}$	1.532(2) Å	1.529(1) Å	1.524(2) Å
a–P^A–$O(3)^A$	120.71°	120.73°	120.81°
b–P^A–$O(3)^A$	90.24°	89.97°	89.84°
c–P^A–$O(3)^A$	143.70°	143.87°	143.86°
Mean	1.535 Å	1.532 Å	1.530 Å
$Ca(1)^A$–$O(1)^{A,B,C}$	2.399(2) Å	2.404(1) Å	2.407(2) Å
a–$Ca(1)^A$–$O(1)^A$	134.44°	134.68°	135.86°
b–$Ca(1)^A$–$O(1)^A$	70.58°	70.21°	67.68°
c–$Ca(1)^A$–$O(1)^A$	44.46°	44.69°	45.89°
$Ca(1)^A$–$O(2)^{D,E,F}$	2.457(2) Å	2.452(2) Å	2.448(2) Å
a–$Ca(1)^A$–$O(2)^D$	131.42°	131.16°	131.81°
b–$Ca(1)^A$–$O(2)^D$	56.09°	56.06°	56.19°
c–$Ca(1)^A$–$O(2)^D$	134.63°	134.81°	134.38°
$Ca(1)^A$–$O(3)^{D,E,F}$	2.807(2) Å	2.802(1) Å	2.793(3) Å
a–$Ca(1)^A$–$O(3)^D$	106.83°	106.86°	107.90°
b–$Ca(1)^A$–$O(3)^D$	16.32°	16.32°	15.39°
c–$Ca(1)^A$–$O(3)^D$	100.09°	100.13°	99.93°
Mean	2.554 Å	2.553 Å	2.549 Å
$Ca(2)^A$–$O(1)^B$	2.701(2) Å	2.711(1) Å	2.901(2) Å
a–$Ca(2)^A$–$O(1)^B$	165.21°	164.11°	162.03°
b–$Ca(2)^A$–$O(1)^B$	74.79°	75.89°	77.97°
c–$Ca(2)^A$–$O(1)^B$	90°	90°	90°
$Ca(2)^A$–$O(2)^C$	2.374(2) Å	2.353(1) Å	2.306(2) Å
a–$Ca(2)^A$–$O(2)^C$	94.00°	93.49°	93.39°
b–$Ca(2)^A$–$O(2)^C$	26.01°	26.51°	26.61°
c–$Ca(2)^A$–$O(2)^C$	90°	90°	90°
$Ca(2)^A$–$O(3)^{F,I}$	2.349(2) Å	2.343(1) Å	2.331(2) Å
a–$Ca(2)^A$–$O(3)^F$	109.91°	109.82°	112.19°
b–$Ca(2)^A$–$O(3)^F$	77.53°	78.32°	77.69°
c–$Ca(2)^A$–$O(3)^F$	159.84°	160.05°	157.74°
$Ca(2)^A$–$O(3)^{A,J}$	2.501(2) Å	2.509(1) Å	2.544(2) Å
a–$Ca(2)^A$–$O(3)^A$	36.22°	35.70°	35.02°
b–$Ca(2)^A$–$O(3)^A$	97.01°	97.74°	98.15°
c–$Ca(2)^A$–$O(3)^A$	119.58°	119.49°	118.92°
$Ca(2)^A$–X	2.3108(7) Å	2.3851(7) Å	2.759(1) Å
a–$Ca(2)^A$–X^A	58.57°	59.09°	63.63°
b–$Ca(2)^A$–X^A	178.57°	171.27°	153.40°
c–$Ca(2)^A$–X^A	90°	81.37°	63.40°
Mean	2.463 Å	2.461 Å	2.493 Å

Note: A = *x*, *y*, *z* (Table 2); B = $-y$, $x - y$, *z*; C = $y - x$, $-x$, *z*; D = $-x$, $-y$, $-z$; E = *y*, $y - x$, $-z$; F = $x - y$, *x*, $-z$; G = $-x$, $-y$, ½ + *z*; H = *y*, $y - x$, ½ + *z*; I = $x - y$, *x*, ½ + *z*; J = *x*, *y*, ½ − *z*; K = $-y$, $x - y$, ½ − *z*; L = $y - x$, $-x$, ½ − *z*.

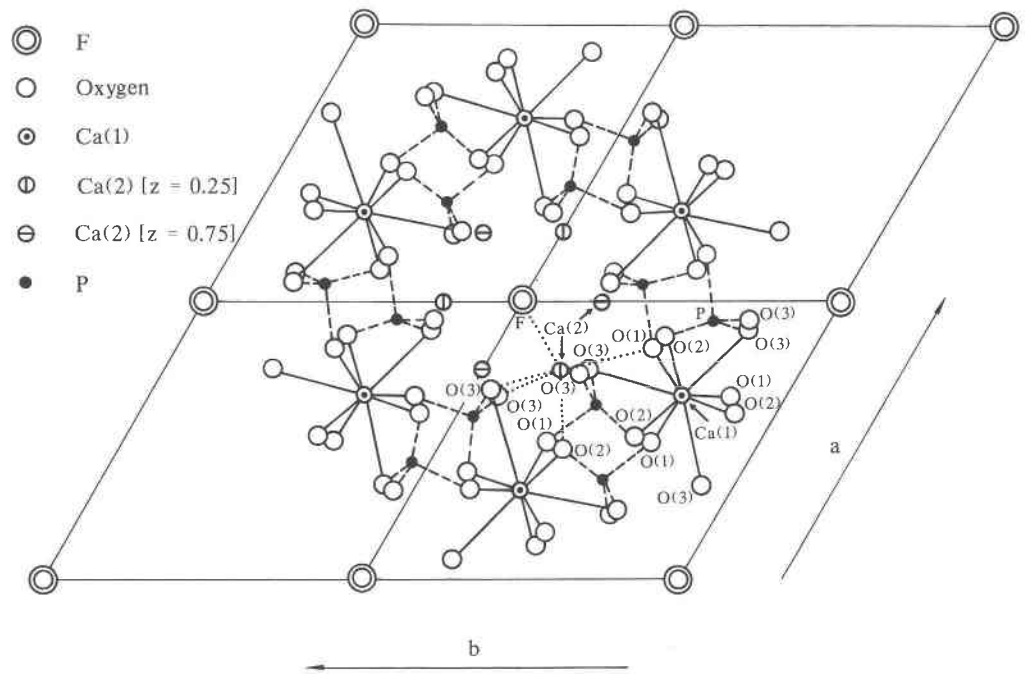

Fig. 1. Schematic depiction of a portion of four unit cells of the apatite structure projected onto the (001) plane (after Bragg and Claringbull, 1965). Solid, dashed, and dotted lines indicate bonds in the different polyhedra.

(7.91 Å^2) for fluorapatite, hydroxylapatite, and chlorapatite, respectively.

Because of its larger size and the longer Ca–Cl bond length as compared to Ca–OH and Ca–F, the Cl anions in chlorapatite are displaced from the (0,0,¼) special position on the mirror plane to two equivalent half-occupied positions at (0,0,0.4323) and (0,0,0.0677). It has been shown (Mackie et al., 1972) that in pure chlorapatite, the Cl anions are all ordered above the plane in a given column and below the plane in adjacent [001] columns along *b*. This ordering yields monoclinic $P2_1/b$ chlorapatite with $b_{mono} = 2 \times b_{hex}$; the monoclinic Cl end-member has been found in nature, as reported by Hounslow and Chao (1970). In the near–end-member hexagonal apatite refined in this study, the column anions are not ordered because no superstructure reflections were observed on precession photos. It is possible, however, that clusters of Cl anions are ordered above or below the plane in a given column, but the sense of ordering can be reversed by F ion "impurities" or anion vacancies, as discussed by Elliott et al. (1973) and Hounslow (1968). Thus the structure may contain regions where the column anions are locally ordered, but overall the average apatite structure has $P6_3/m$ symmetry (Fig. 3). In chlorapatite, the Cl anion is displaced so far from the mirror plane (1.2 Å) that a weak bond (0.09 valence units) forms between Ca(2) and a second Cl anion, Cl′, located one-half unit cell away along *c* [Ca(2)–Cl′ bond distance = 3.27 Å]. The slight overbonding of Ca(2) because of this weak Ca(2)–Cl′ interaction is balanced through reduced bonding between Ca(2) and O(1) in chlorapatite.

Kay et al. (1964) refined the crystal structure of hydroxylapatite using three-dimensional X-ray ($R = 0.075$) and neutron ($R = 0.055$) data. They determined that the OH anions are disordered, half-occupying equivalent (0,0,*z*) positions 0.35 Å above and below the mirror planes. It has been suggested (Elliott et al., 1973) that if insufficient F anions or vacancies (<0.15 per site?) exist in the anion columns, OH anions will order above the plane in a given column and below the plane in the adjacent column along *b*, again giving rise to monoclinic $P2_1/b$ symmetry with $b_{mono} = 2 \times b_{hex}$. In our diffraction experiments, long-exposure precession photographs and diffractometer scans showed no evidence of the monoclinic superstructure.

The arrangement of hydroxyls in the [001] columns of the hydroxylapatite structure is shown schematically in Figure 3. Clusters of hydroxyls exist that are ordered above and below the mirror plane. In natural hydroxylapatites, however, enough F "impurities" or anion vacancies exist in a single column to act as "reversal" sites, thus giving rise to a locally ordered structure that averages to the disordered $P6_3/m$ model.

Implications for ternary apatites

Apatite minerals with the formula $Ca_5(PO_4)_3X$ (X = F, OH, Cl) have long been considered as miscible isostructures even though few crystal-structure refinements have been published on binary or ternary members of the system. Observations on the hexagonal near–end-members apatites of this study, however, clearly demonstrate that the structural configurations of the column anions (F, Cl,

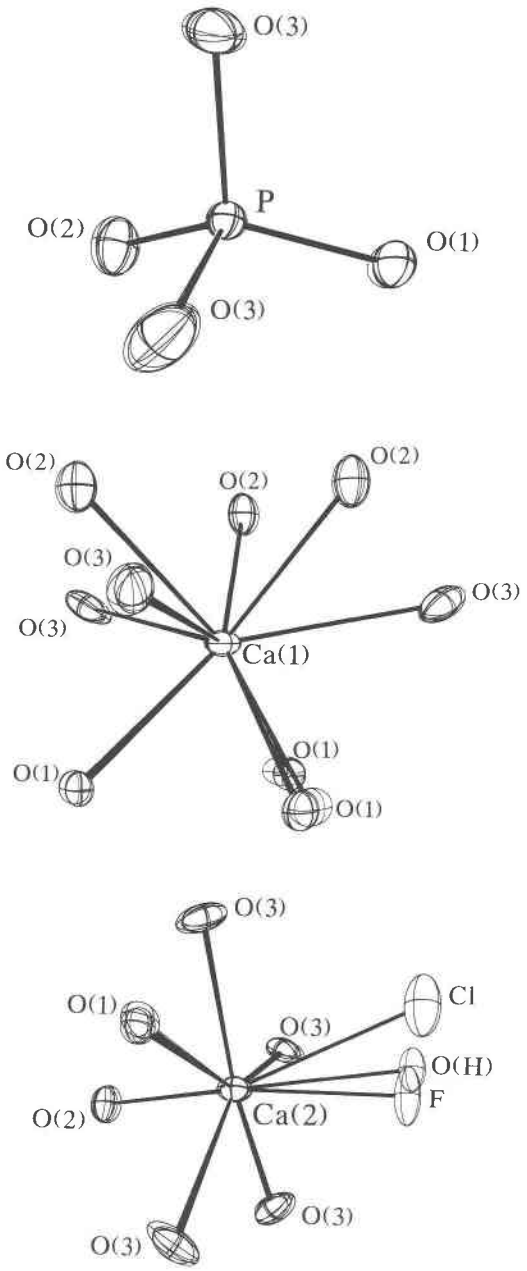

Fig. 2. ORTEP (Johnson, 1965) drawings of PO_4 tetrahedra and Ca(1) and Ca(2) polyhedra for the three apatite structures. Each overlay is a superposition of the analogous polyhedra from the three end-member structures drawn to the same scale and with coincident central cations.

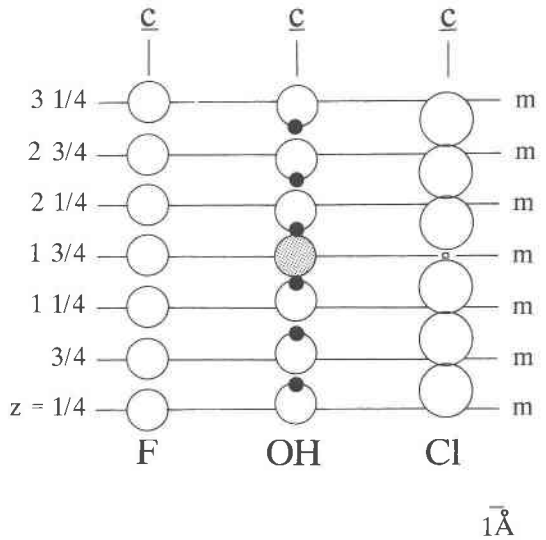

Fig. 3. Depiction (to scale) of anion columns in hexagonal fluorapatite, hydroxylapatite, and chlorapatite. Column "F" shows F anions in fluorapatite located on mirror planes at z = ¼, ¾ in successive unit cells. Column "OH" depicts three successive hydroxyls in hydroxylapatite disordered 0.35 Å *above* the mirror planes and three successive hydroxyls disordered *below* the mirror planes, with the sense of disordering reversed by an F anion (stippled) "impurity" at z = 1¾. Column "Cl" shows three successive Cl anions in chlorapatite disordered *above* the mirror planes and three successive Cl anions disordered *below* the mirror planes. The vacancy (□) at z = 1¾ in chlorapatite must exist in order to reverse the sense of ordering, as F and OH species are prohibited. Radii: F = OH = 1.4 Å, Cl = 1.7 Å. Scale of H atom (solid circles) is arbitrary. Scale bar = 1 Å.

OH) are not miscible. In this section, we develop further structural constraints that must govern binary and ternary solution of apatites.

Consider, for example, a hypothetical binary apatite with the composition $Ca_5(PO_4)_3(OH_{0.5}Cl_{0.5})$. If we assume that the anion positions in this binary apatite are the same as in the end-members, then its structure would have anion columns that contain both Cl and OH anions that are, on the average, disordered about the mirror plane. In any column there are thus four possible anion sites associated with each mirror plane: an OH site located 0.35 Å below the plane, an OH site 0.35 Å above the plane, a Cl site 1.2 Å below the plane, and a Cl site 1.2 Å above the plane. On average, each of these four possible sites would be one-fourth occupied by its respective occupant, OH or Cl. Anion-anion distances (Fig. 4) calculated for column anions using end-member data preclude such a disordered $P6_3/m$ arrangement, however.

Examination of possible anion arrangements and Cl–OH interionic distances demonstrates why complete disordering is not possible. For example, associated with one-fourth of the mirror planes at z = ¼ we would find a Cl anion disordered 1.2 Å above the plane. In this model, possible neighbors along $+c$ include an OH anion *below* the adjacent plane at z = ¾ [Cl–OH distance = 1.81 Å], an OH anion *above* the adjacent plane [Cl–OH distance = 2.52 Å, whereas ideal non-hydrogen-bonded Cl–O distance = 3.2 Å], a Cl anion *below* the adjacent plane (Cl–Cl distance = 0.92 Å), and a Cl anion *above* the adjacent plane, at a distance of $c/2$ = 3.41 Å. Only the last configuration (Cl anions above the plane, ad infinitum) is reasonable based on interionic distances. Vacancies can, of

Anion Associated With Mirror Plane at z = 0.75

Anion Associated With Mirror Plane at z = 0.25

	OH_a	OH_b	Cl_a	Cl_b
OH_a	3.41	2.70	4.30	1.81
OH_b	4.12	3.41	5.01	2.52
Cl_a	2.52	1.81	3.41	0.92
Cl_b	5.01	4.30	5.90	3.41

Fig. 4. Anion-anion distances (Å) for column anions using end-member data presented in this paper. Subscript "a" indicates anion disordered *above* the associated mirror plane, subscript "b" indicates anion disordered *below* the associated mirror plane. Shaded cells indicate configurations prohibited because of unreasonably short interionic distances or juxtaposition of H ions. All values were calculated assuming c = 6.83 Å, the average of c_{OH} and c_{Cl}.

course, initiate a new anion sequence in the column, although it has not been established that *stoichiometric* vacancies exist in ternary apatites, nor how charge balance would be maintained. This simple binary example can be extended to ternary members including F anions in the mirror plane, as well, because the Cl–F distance (2.17 Å) would lie between the two Cl-OH values described above. It is thus clear that the ternary members of the apatite system are not ideal solutions of the hexagonal end-members. There are several possible ways, however, that ternary solid solution can be accommodated. Extensive rearrangement of the end-member anion configuration, as yet undefined, may occur in the ternary system to accommodate the Cl ion; anion vacancies may also play an *essential* role in stabilizing these apatite structures. Finally, a completely disordered hexagonal structure may be realized where there is anion ordering *within* individual columns, but disordering among the columns themselves.

In a newly initiated study, we are analyzing the crystal structures of binary and ternary apatites in the OH-F-Cl system. Limited data obtained to date indicate that binary and ternary apatites respond to solid solution in at least two ways: (1) by large (~0.4 Å) shifts of anion positions relative to the end-members and (2) by reduction of *ternary* apatite symmetry to monoclinic, where Ca(2) and the column anions are no longer constrained by the hexagonal symmetry elements, and thus a variety of anion sites suitable for the three anions in ternary apatites are created.

Acknowledgments

We thank I. D. Brown for kindly providing constants for calculation of Ca–Cl bond strengths. This work was supported by grants from the National Science Foundation (CHE-8418897 and EAR-8717655 to Hughes and EAR-8517621 to Crowley and Cameron). Specimens used in this study were provided by George E. Harlow of the American Museum of Natural History and P. J. Dunn of the National Museum of Natural History, Smithsonian Institution. The manuscript was improved by thorough reviews by G. Y. Chao and R. C. Rouse.

References cited

Beevers, C.A., and McIntyre, D.B. (1946) The atomic structure of fluorapatite and its relation to that of tooth and bone material. Mineralogical Magazine, 27, 254–257.

Bragg, L.B., and Claringbull, G.F. (1965) Crystal structures of minerals, 409 p. G. Bell and Sons, London.

Boudreau, A.E., and McCallum, I.S. (1987) Halogens in apatites from the Stillwater Complex: Preliminary results (abs.). EOS, 68, 1518.

Candela, P.A. (1986) Towards a thermodynamic model for the halogens in magmatic systems: An application to the melt-vapor-apatite equilibria. Chemical Geology, 57, 289–301.

Crowley, K.D., and Cameron, M. (1987) Annealing of etchable fission-track damage in apatite: Effects of anion chemistry. Geological Society of America Abstracts with Programs, 19, 631–632.

Elliott, J.C., Mackie, P.E., and Young, R.A. (1973) Monoclinic hydroxylapatite. Science, 180, 1055–1057.

Frenz, B.A. (1985) Enraf-Nonius structure determination package. SDP users guide, Version 4. Enraf-Nonius, Delft, The Netherlands.

Green, P.F., Duddy, I.R., Gleadow, A.J.W., Tingate, P.R., and Laslett, G.M. (1986) Thermal annealing of fission tracks in apatite 1. A qualitative description. Chemical Geology, 59, 237–253.

Hounslow, A.W. (1968) Crystal structures of two naturally occurring chlorapatites. Ph.D. dissertation, Carleton University, Northfield, Minnesota.

Hounslow, A.W., and Chao, G.Y. (1970) Monoclinic chlorapatite from Ontario. Canadian Mineralogist, 10, 252–259.

Johnson, C.K. (1965) A FORTRAN thermal ellipsoid plot program for crystal structure illustrations. U.S. National Technical Information Service, ORNL-3794.

Kay, M.I., Young, R.A., and Posner, A.S. (1964) Crystal structure of hydroxylapatite. Nature, 204, 1050–1052.

Mackie, P.E., Elliott, J.C., and Young, R.A. (1972) Monoclinic structure of synthetic $Ca_5(PO_4)_3Cl$, chlorapatite. Acta Crystallographia, B28, 1840–1948.

Mehmel, M. (1930) Über die Struktur des Apatits. I. Zeitschrift für Kristallographie, 75, 323–331.

Náray-Szabó, S. (1930) The structure of apatite $(CaF)Ca_4(PO_4)_3$. Zeitschrift für Kristallographie, 75, 387–398.

Stormer, J.C., and Carmichael, I.S.E. (1971) Fluorine-hydroxyl exchange in apatite and biotite: A potential igneous geothermometer. Contributions to Mineralogy and Petrology, 31, 121–131.

Sudarsanan, K., Mackie, P.E., and Young, R.A. (1972) Comparison of synthetic and mineral fluorapatite, $Ca_5(PO_4)_3F$, in crystallographic detail. Materials Research Bulletin, 7, 1331–1338.

Young, E.J., Myers, A.T., Munson, E.L., and Conklin, N.M. (1969) Mineralogy and geochemistry of fluorapatite from Cerro de Mercado, Durango, Mexico. U.S. Geological Survey Professional Paper 650-D, D84–D93.

Manuscript received October 14, 1988
Manuscript accepted March 7, 1989